Available online at www.sciencedirect.com
SCIENCE DIRECT
Polymer 46 (2005) 3385–3393
polymer
www.elsevier.com/locate/polymer

Oriented structure of PP/LLDPE multilayer and blends films

X.M. Zhang, A. Ajji*

Industrial Materials Institute, National Research Council Canada, 75 boul. de Mortagne, Boucherville, Québec, Que., Canada J4B 6Y4

Received 19 November 2004; received in revised form 22 February 2005; accepted 2 March 2005
Available online 21 March 2005

Abstract

Polypropylene/linear low-density polyethylene (PP/LLDPE) multilayer and blends blown films are investigated in terms of crystalline morphology and orientation. The crystalline structures were probed using microscopy, infrared trichroism and X-ray pole figures. Two different PPs were used, one was a homopolymer and the other was a copolymer. Similar orientation characteristics were observed for both PP components in the blends and multilayer films, the PE component, however, showed very different structure, especially for the crystalline *a*- and *b*-axes orientation. The row-nucleated structure, epitaxial crystallization and transcrystallization observed in the films are discussed.

Keywords: Morphology; Orientation; Polypropylene–polyethylene films

1. Introduction

Flow-induced crystalline morphology and orientation of semi-crystalline polymers is of great importance to many polymer processes such as injection moulding, film blowing, fiber spinning, etc. In these processes, the molten polymers are subjected to shear and elongational flow fields and crystallize during or subsequent to the imposition of flow. The intense shearing flows (e.g. injection moulding) or elongation flows (e.g. film blowing) have tremendous effect on crystalline morphologies and, therefore, on the final product properties. In fact, the semi-crystalline flow-induced morphology developed in the final product is very different from the spherulitic one developed under quiescent crystallization conditions. The elongational flow promotes fibrillar-like structure oriented in the stress direction that serves as nucleation for radial growth of chain-folded lamellae perpendicular to stress direction [1]. The row-nucleated structure proposed by Hill and Keller [2] has been widely used to describe elongational flow-induced crystallization morphology. Shish-kebab structure is formed by shear flow, where the full extension of chains is prohibited, but the extension of portions of chains can occur [3]. For blown films, the earliest stages of polymer crystallization under flow or stress provide valuable data regarding microscopic origin of the effects of flow on the overall crystallization kinetics and morphology [4].

On the other hand, for dissimilar polymers, specific interactions at an interface may induce particular crystallization features at the interface. Heteroepitaxy is one of the well-known behaviours of polymer-oriented crystallization [5]. Epitaxial crystallization has been found between immiscible crystalline polymer pairs, in which one phase epitaxially crystallizes on the other first crystalline phase. Great interest was dedicated to studies between helical chain polymers such as polypropylene (PP) and zigzag chain polymer, such as polyethylene (PE) [6,7], polyesters [8,9], and polyamide [8]. PE showed epitaxial arrangement crystallization on oriented α-PP substrate; the PE chains were oriented at angles of about 50° apart from PP chain direction [7,10,11]. This was attributed to the parallel alignment of PE chains onto the oblique methyl group rows in the lateral ac contact plane of α-PP with 0.5 nm intermolecular distance for chain row matching [8].

Transcrystallization is another type of crystallization behaviour that may occur at the interface between two semi-crystalline polymers. It consists in a lamellar growth of one polymer nucleated from the interface (lamellae perpendicular to the interface). It may result from various reasons: (1) crystallization temperature difference between the two

* Corresponding author. Tel.: +1 450 641 5244; fax: +1 450 641 5105.
E-mail address: abdellah.ajji@cnrc-nrc.gc.ca (A. Ajji).

0032-3861/$ - see front matter
doi:10.1016/j.polymer.2005.03.004

polymers [12]; (2) the presence of stresses at the interface causing many nucleating sites [13]; and (3) crystal unit cell or chemical structure similarities between the two polymers [5,14,15].

Polyolefins blends and multilayer films are widely used in flexible packaging. Different process and resin parameters may significantly affect their structure and hence, properties. The advantage of using PP in such films will enhance films stiffness, strength and temperature useful range. Special interactions at PP/PE interfaces can result in PE crystallization on PP surface in a specific manner, as discussed above. Several experiments studied those crystallization structures by using particular PP/PE film preparation processes [6,7,10,11]. However, those processes were very different from the blown film process. The complex stress and flow history experienced in the blown film process makes it hard to automatically infer the crystalline morphology.

It is hence the objective of this work to study the crystalline structure and orientation of PP/PE blown films. Films made from PP/PE blends and multilayered ones will be evaluated. Specifically, we will examine the orientations and crystalline morphologies in polypropylene/linear low-density polyethylene (PP/LLDPE) blend and multilayer films, using a PP homopolymer and a PP copolymer. We will determine and discuss for each case and each polymer the crystalline structure type (row-nucleated or else) and the type of growth at the interface: epitaxial and/or transcrystalline.

2. Experimental

2.1. Materials and blown films preparation

The characteristics of the materials used in this study are listed in Table1. Nova Chemical Inc., provided the octene based Ziegler–Natta catalyzed LLDPE, traded under the name EX-FG120-A05. The molecular characteristics of the LLDPE were kindly provided by the manufacturer. Two polypropylenes provided by Basell Company were used. The first one, denoted as PP-1, was a polypropylene homopolymer (trade name Pro-fax PDC 1280) and the second (PP-2) a polypropylene copolymer (trade name Pro-fax-SR257M). The latter was a clarified PP random copolymer resin with ethylene, for which we could not obtain the ethylene content. The molecular weight characteristics for the PP's were determined by GPC after dissolution in trichlorobenzene at 135 °C and using polystyrene standards.

The films were oriented as much as possible in machine direction. Thus, high draw-down ratio (DDR), medium blow up ratio (BUR) and low frost-line height (FLH) were used in this work. The films were produced using a 5-layer Brampton engineering extrusion blowing line. The output was fixed at 10 kg/h, DDR at 25 and the BUR at 2.0. The die gap (1.1 mm) and die temperature (250 °C) were fixed for all the films. All the films were prepared with the same thickness of 25 μm. Layout and compositions of the blend and multilayer films are given in Table 2.

2.2. FT-IR trichroism

Measurements were carried out on a Nicolet 170SX FT-IR apparatus at a resolution of 2 cm^{-1} with an accumulation of 128 scans. Polarization of the beam was done using a zinc selenide wire grid polarizer from spectra-tech.

Specimen were put perpendicular to the FT-IR beam with a vertical machine direction and horizontal transverse direction, and the measurements were performed with radiation polarized in the machine and transverse directions, respectively. This allows the determination of spectra for the machine (S_M) and transverse (S_T) directions. The normal spectrum was obtained using the tilted method and the spectrum for the thickness direction (S_N) was calculated. A refractive index of 1.51 for PP was used and the isotropic spectrum was calculated by $S_0 = 1/3(S_M + S_T + S_N)$. The detailed calculation procedure can be found in Refs. [16,17].

Typical FT-IR spectra for both PP and LLDPE are shown on the same graph in Fig. 1. No overlap between their vibrations can be seen in the wave number range of interest. Spectra portions of interest in the case of LLDPE and PP are

Table 1
Polymer resins used in this work and some of their characteristics

Resin	M_n (kg/mol)	M_w (kg/mol)	M_w/M_n	Comonmer content (mol%)	MI for LLDPE or MFR for PP (g/10 min)	Density (g/cc)	T_m (°C)	T_c (°C)
LLDPE	31,000	103,000	3.4	5.4	1.0	0.920	122.0	104.0
PP-1 (PP homopolymer, profax PDC 1280)	135,000	420,000	3.1	None	1.20	0.902	163.0	112.0
PP-2 (PP random copolymer, profax SR257M)	101,000	346,000	3.4	Unknown	2.00	0.902	143.0	118.0

Table 2
Layout and compositions of the blown films used in this work

Code	Layout and compositions of the blown films
Pure materials	
LLDPE	LLDPE/LLDPE/LLDPE/LLDPE/LLDPE = 15/25/20/25/15
PP-1	PP-1/PP-1/PP-1/PP-1/PP-1 = 15/25/20/25/15
PP-2	PP-2/PP-2/PP-2/PP-2/PP-2 = 15/25/20/25/15
Blow films of 50/50 LLDPE/PP blends	
Blend1 (PP-1 with LLDPE)	Blend-1/blend-1/blend-1/blend-1/blend-1 = 15/25/20/25/15
Blend2 (PP-2 with LLDPE)	Blend-2/blend-2/blend-2/blend-2/blend-2 = 15/25/20/25/15
Multilayer films	
5-layer1	PP-1/LLDPE/PP-1/LLDPE/PP-1 = 15/25/20/25/15
5-layer2	PP-2/LLDPE/PP-2/LLDPE/PP-2 = 15/25/20/25/15

shown on Fig. 2(a) and (b), respectively. Of the PP vibrations, those at 809, 900, 1100 and 1220 cm^{-1} show perpendicular polarization characteristics, whereas those at 841, 973, 998, 1153, 1167 and 1256 cm^{-1} show parallel dipole moment orientation. The 841 cm^{-1} vibration is well referenced and associated with the PP crystalline phase [18,19] and 1153 cm^{-1} was assigned to the amorphous phase [20]. The 973 cm^{-1} vibration was observed to be associated with both crystalline and amorphous phases [21]. The 1256 cm^{-1} is a mixed vibration (amorphous and crystalline phase), having a transition moment angle with chain axis of 38.5° [22]. The 840, 998 and 1165 cm^{-1} are among the strong vibrations and are associated with α-PP helical crystal. The 840 cm^{-1} was shown to be especially sensitive to smectic region orientation, and 1165 cm^{-1} is very close to the amorphous peak 1153 cm^{-1}. To obtain precise measurements for the crystalline chain orientation, 998 cm^{-1} vibration was adopted in this work. For the orientation of the amorphous phase, 1153 cm^{-1} was not used because of overlapping with the crystalline vibration at 1165 cm^{-1} (in fact, erroneous results were observed, e.g. values lower than −0.5 or summation of orientation factors different from 0) and no amorphous orientation results are reported for PP.

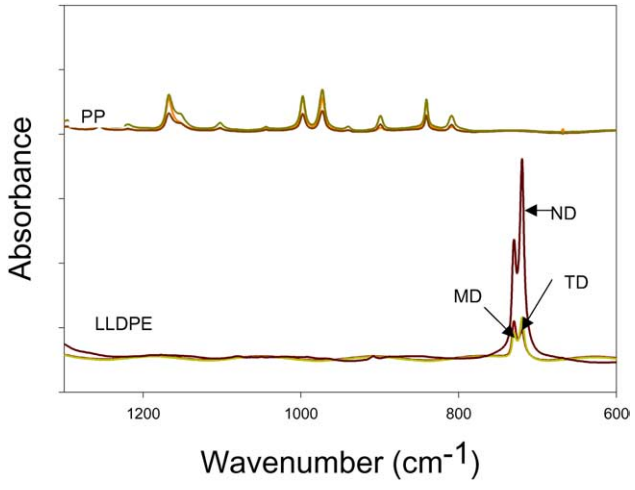

Fig. 1. Polarized FT-IR spectra of pure LLDPE and PP-1 blown films in different directions as indicated.

FT-IR orientation functions is usually determined using two characteristic angles ϕ and α. ϕ is the angle the polymer chain axis makes with the reference direction, and α is the angle that the transition moment makes with the polymer chain axis. When α is known, the orientation function can be calculated. The PP chain axis orientation function with respect to a given sample direction J (where $J = M, T, N$) can be determined from the trichroism of a specific peak in IR spectra by Refs. [16,17]:

$$f_J = \frac{(A_J/A_0 - 1)}{(3\cos^2\alpha - 1)} \quad (1)$$

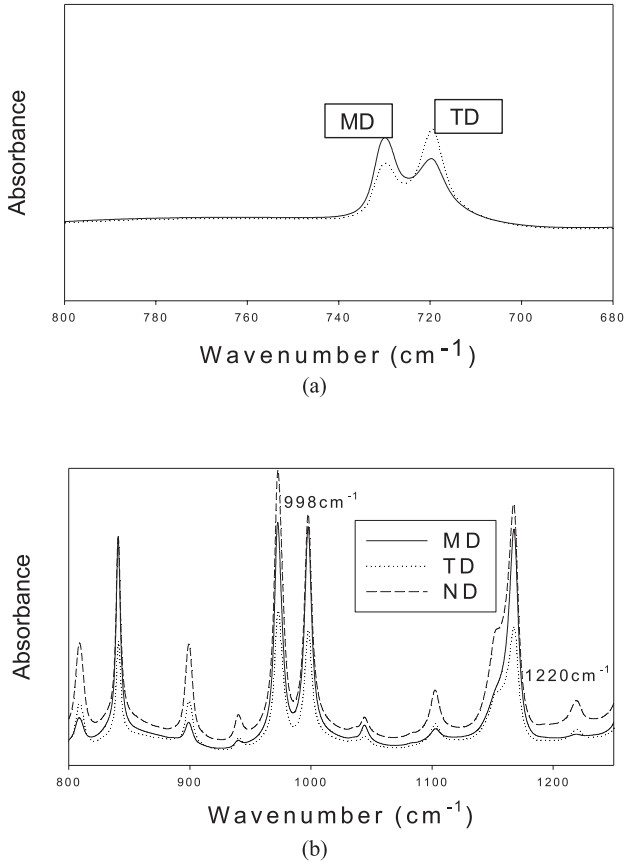

Fig. 2. FT-IR spectra for pure LLDPE (a) and pure PP-1 (b) blown films in the spectral region of interest.

where A_J is intensity (we usually use the area under the peak) of the vibration of interest in the spectrum S_J, A_0 the intensity of the same vibration in the isotropic spectrum. The orientation function for the crystalline *c*-axis was calculated using 998 cm^{-1}, for which the value of α was taken as 18°, can be written as [23]:

$$f_J = 0.58(A_J/A_0 - 1) \quad (2)$$

For LLDPE, orientation measurements and discussion using this FT-IR technique has already been extensively discussed [16,17]. The peaks used were 730, 720 and 722 cm^{-1} which are associated with crystalline *a*-axis, crystalline *b*-axis and amorphous, respectively. These peaks are well separated from those of PP as already shown above. The accuracy and reliability of these vibrations for the determination of orientation factors is discussed elsewhere [24]. Since, PP and PE WAXD diffraction overlap in a certain range of 2θ, it is hard to obtain both PP and PE's orientation using this technique, especially for PE component in the blends and multilayer films. FT-IR compensates this disadvantage of WAXD and allows determination of PE orientation factors. WAXD is used to determine the PP crystalline factors (as described below) in order to compare them with those from FT-IR.

2.3. Wide angle X-ray diffraction

The crystalline axes orientation factors were determined from wide-angle X-ray diffraction pole figures of crystalline reflections using a Bruker AXS X-ray goniometer equipped with a Hi-STAR two-dimensional area detector. The generator was set up at 40 kV and 40 mA and the copper K_α radiation ($\lambda = 1.542$ Å) was selected using a graphite crystal monochromator. Sample to detector distance was fixed at 8 cm. Film samples were stacked to a thickness of about 3 mm in order to obtain enough accuracy in a reasonable time. The MD, TD and ND WAXD patterns were measured by cutting the film stacks having sections with desired orientations. For PP films, diffraction from the (110) or (040) planes were used and their pole figures determined. Angular steps of 3° were used. As there is no reflection associated with (001) planes (*c*-crystallographic axis) in the PP α phase, these were calculated from the diffraction intensities of (110) and (040) planes based on the unit cell geometry [25]:

$$\langle \cos^2\phi_{c,J} \rangle = 1 - 1.099\langle \cos^2\phi_{110,J} \rangle - 0.901\langle \cos^2\phi_{040,J} \rangle \quad (3)$$

2.4. Crystalline morphology

The lamellar morphologies were observed using a low voltage field emission scanning electron microscope (FE-SEM S-4700) from Hitachi. This provides a high resolution of 2.5 nm at a low accelerating voltage of 1 kV and a resolution of 1.5 nm at 15 kV with magnification from 20× to 500k×. The advantage of FE-SEM S-4700 is that the crystalline morphology can be directly observed without any chemical treatment on the samples and minimal coating (or not at all). The multilayer films were microtomed and etched for 20 min, then the cross section observed.

3. Results and discussions

3.1. Morphologies and orientation of LLDPE films

The detailed characterization, morphology and orientation of pure LLDPE were reported in our previous study [17]. The main result is summarized in Fig. 3: the LLDPE developed a spherulitic crystalline morphology. The orientation results showed *a*-axis orientation in MD and no preferential *c*-axis orientation.

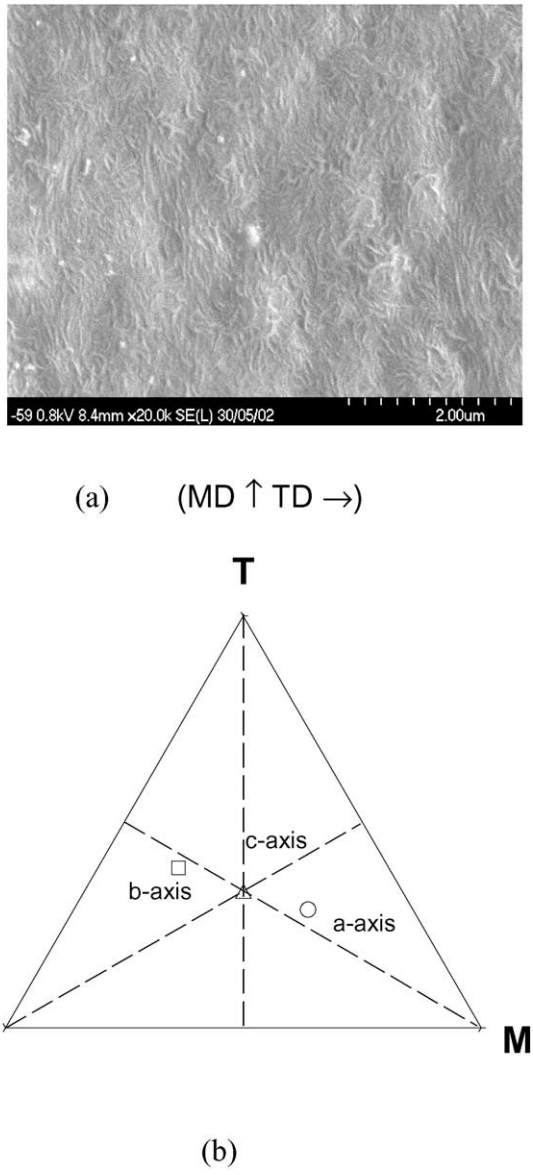

Fig. 3. Morphology (a) and orientation (b) for pure LLDPE blown film.

3.2. Morphologies and orientation of PP-1 and PP-2 films

WAXD θ–2θ plot in Fig. 4 for pure PP-1 and PP-2 blown films shows that both films have the same crystalline α (monoclinic) form. The complete 2D WAXD pattern for those same films is shown in Fig. 5. They exhibit four sharp crystalline ring reflections: the inner most ring is (110), the one next to it is (040), the third one (130), the outer most is $(111)+(\bar{I}31)$. The ND–MD and TD–MD planes patterns are similar, and different from the ND–TD one. The (040) reflection is observed as an arc in both ND–MD and TD–MD patterns (with more intense spot in the ND–MD one) and as a ring in the ND–TD pattern. This suggests that the *b*-axis is mostly located in the TD–ND plane, perpendicular to the machine direction MD.

Pole figures (not presented here) also indicated that the (040) pole is concentrated in the direction perpendicular to the machine direction, and has more intensity in the normal direction. The (110) reflection was found concentrated in the band making an angle of about 40–50° to MD. The *b*-axis orientation could be computed directly from the (040) intensity distribution. The orientation factors of crystalline *b*- and *c*-axes are shown in a triangle plot in Fig. 6. The molecular chains are oriented in the MD, and *b*-axis shows orientation perpendicular to MD.

The crystalline *c*-axis orientation from WAXD is a calculated value. It can also be directly measured from FT-IR as discussed in the experimental section and is shown also in Fig. 6. *c*-axis orientation toward machine direction was observed for both PP-1 and PP-2 blown films, which is consistent with WAXD pole figure results, but the orientation factor magnitude are larger than the one from WAXD pole figure. This discrepancy in the values of measured *c*-axis orientation may be due to different factors such as the some contribution of the amorphous phase, peak deconvolution, etc. as discussed elsewhere for PE [24].

PP-1 morphologies are shown in Fig. 7. A high level of row-nucleated structure is not observed here, but PP-1 do shows some lamellar alignments in the perpendicular direction. Etching allows accessing the bulk morphology

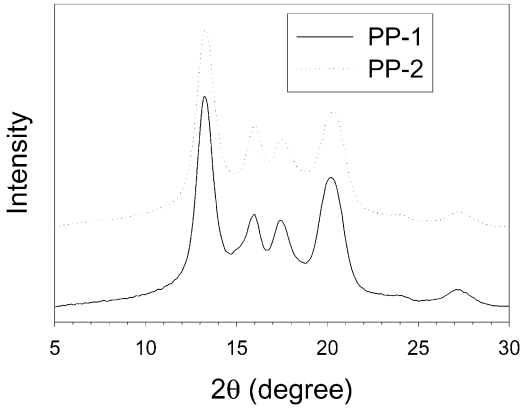

Fig. 4. WAXD θ–2θ plot for pure PP-1 and PP-2 blown films.

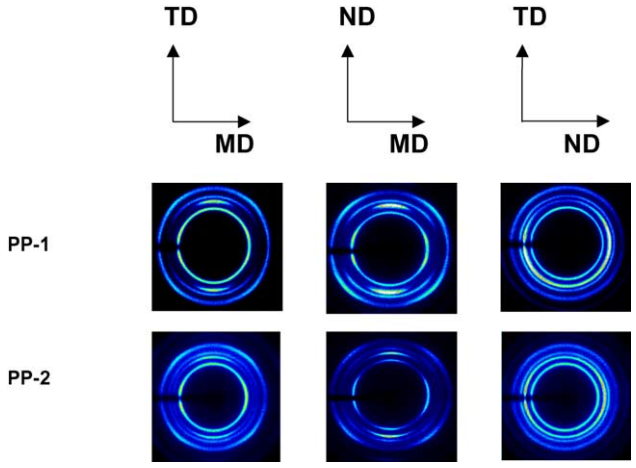

Fig. 5. WAXD patterns for pure PP-1 and PP-2 blown films.

by reducing the thickness. The PP-1 film etched of 20 min shows some sheaf-like crystalline morphology. The sheaf like structure resulted from anisotropy of crystal growth; molecular orientation in the melt causes faster growth of lamellae perpendicular to flow direction than parallel to it. The sheaf-like morphology is not observed to initiate on the surface morphology. This is probably due to the fast cooling at the surface compared to the bulk through the film thickness. The oriented melts at the outer surface are less relaxed so that more row-nucleated like morphology is formed. The PP lamellar morphology seen here is different from the PE lamellar arrangements [16,17]. Lamellar branching is observed in both surface morphology and sheaf-like bulk morphology. The lamellar branching from the primary lamellae is produced by epitaxial growth due to cross-hatched lamellar texture, which is a unique habit of PP crystalline structure. The lamellar morphology was more random for PP-2 (not shown), probably due to faster relaxation in the melt and lower orientation.

In conclusion of the morphological observations for both PPs is that no significant level of row-nucleated structure

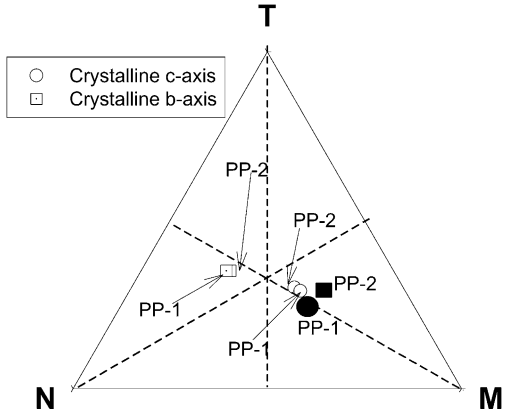

Fig. 6. Orientation factors obtained for pure PP-1 and PP-2 blown films: open symbols from WAXD and filled symbols for *c*-axis orientation from FT-IR.

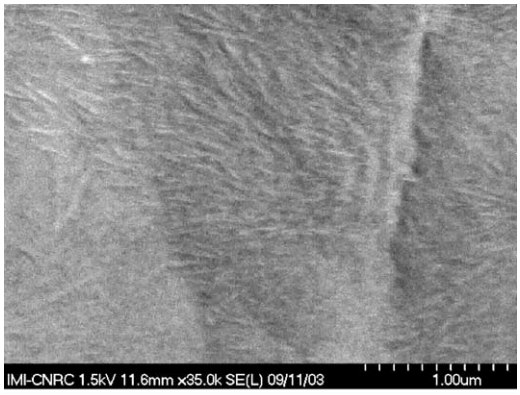

(a)

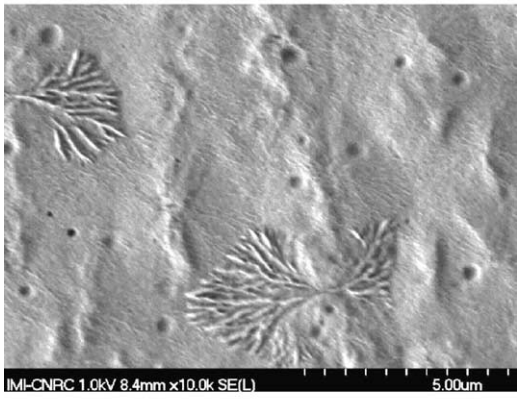

(b)

Fig. 7. PP-1 morphologies (a) without etching (b) with 20 min etching.

was observed for PP films produced by blowing process. Even for an extremely high melt strength PP, no columnar row-nucleated structure was found [26]. Two steps are critical for the final film morphology: orientation-induced structure (nuclei) in the melt at the pre-crystallization stage and subsequent morphological development based on the first stage nuclei. The fast relaxation time is one of the reasons for the low level of row-nucleated structure in PP. Another reason may be due to the cross-hatched lamellar texture, which results in lamellar branching, a characteristic of monoclinic crystalline unit cell of i-PP.

3.3. Morphologies and orientations of LLDPE/PP-1 blends and multilayer films

The PP-1 orientation in the blend and multilayer films from WAXD pole figures and FT-IR is shown in Fig. 8. PP-1 shows *c*-axis orientation in MD and *b*-axis orientation in perpendicular directions for both blend and multilayer film, as can be observed on Fig. 8. This is similar to the results obtained on pure PP-1 blown films discussed above. The LLDPE crystalline axes orientation from FT-IR is shown in

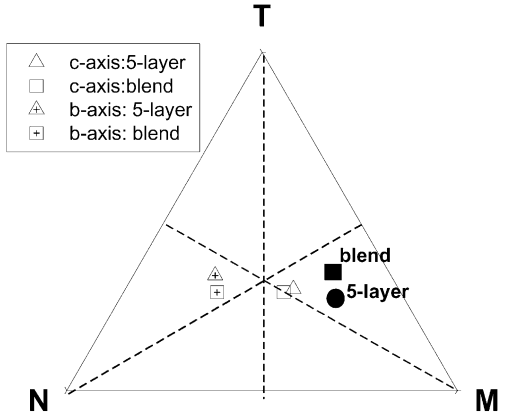

Fig. 8. Orientation functions obtained from X-ray (open symbols) and from FT-IR (filled symbols, *c*-axis only) for the PP-1 components in blends and 5-layer films.

Fig. 9. The LLDPE in multilayer film shows the similar orientation results as pure LLDPE does: *a*-axis orientation toward MD, *b*-axis in TD–ND plane and random *c*-axis. In the blend, however, LLDPE shows an *a*-axis orientation in the thickness direction (ND), and both *b*-axis and *c*-axis orient in the half way between MD and TD in the MD–TD plane, significantly different from its behaviour in the multilayer film, despite the uncertainties in the quantitative values.

The morphology of LLDPE blends with PP-1 is shown in Fig. 10. Since, polymers are crystalline, the phase contrast between the two phases is weak, but the two phases can be distinguished by their different lamellar morphologies by taking into account their orientation characteristics as determined from WAXD and/or FT-IR. PP-1 orientation is similar to that in the pure or multilayer films, i.e. mostly isotropic or low orientation levels, which indicate no particular orientation of lamellae. LLDPE, however, shows a strong orientation of the *a*-axis in the normal direction, a trend significantly different from pure LLDPE as well as PP and is indicative of preferential orientation of

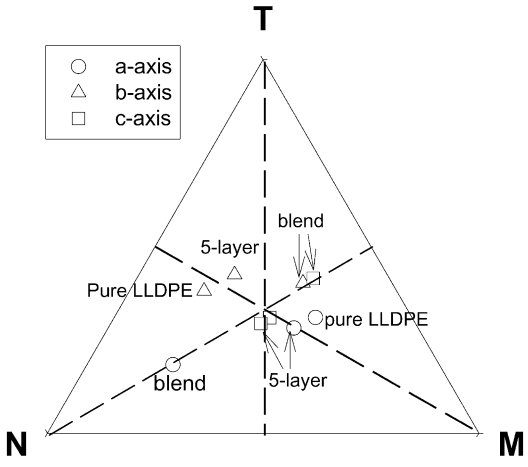

Fig. 9. The orientations of crystalline phases of LLDPE component in the blend and 5-layer films using PP-1. Measured by FT-IR.

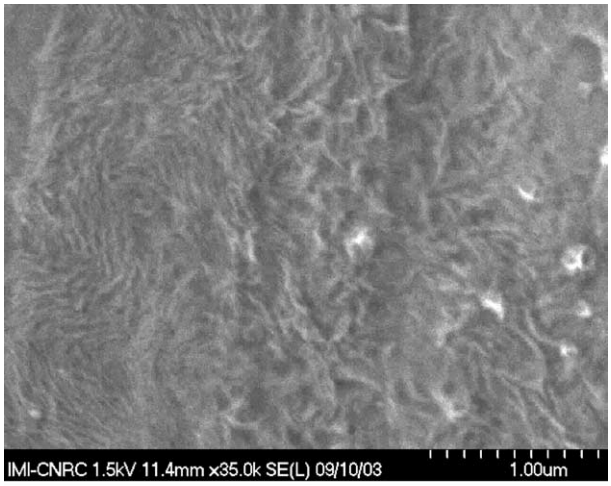

(a)

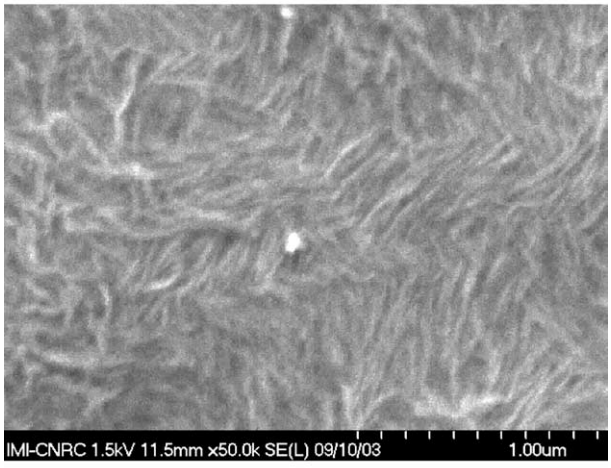

(b)

Fig. 10. Morphologies of LLDPE/PP-1 blend: (a) the zone showing both phases (b) higher magnification showing LLDPE epitaxial crystallization.

the LLDPE lamellae. This is interpreted here as due to epitaxial crystallization of LLDPE onto PP-1 and results in lamellae oriented 40–50° to MD. The LLDPE chains around the interface alternately stacked having *c*- and *b*-axes oriented in MD–TD plane, this epitaxial crystalline structure was seen only in MD–TD plane, suggested by PE's *c*- and *b*-axes orientation in MD–TD plane.

The interfacial morphology for PP-1/LLDPE multilayer films (5-layer) is shown in Fig. 11. For an epitaxial nucleation, LLDPE crystal orientation develops along MD–TD plane but also possibly along ND [27], in which case it would be transcrystalline morphology. From the figure, neither cross-hatched epitaxial crystalline structure nor transcrystalline layers are observed in the thickness direction for the LLDPE lamellae. The lack of transcrystalline morphology in this case could be due to chemical or physical differences (for example, lamellar dimensions) and the small difference in crystallization temperature between PP-1 and LLDPE [28]. For the cross-hatched epitaxial crystallization for i-PP/PE multilayer films, the PE epitaxial crystallization formed as a thin PE layer next to PP in the MD–TD plane instead of thickness direction, as reported in most studies on the epitaxial morphology of PP/PE multilayered films [6,7,10,11].

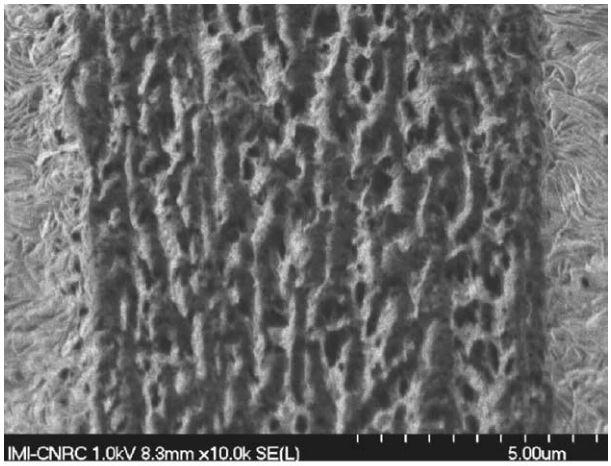

(a)

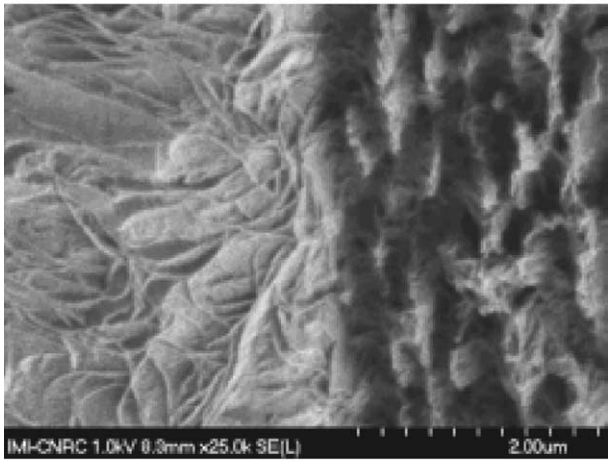

(b)

Fig. 11. Interfacial morphology of PE/PP-1 multilayer film to different magnifications.

3.4. Morphologies and orientations of LLDPE/PP-2 blends and multilayer films

The PP-2 orientation in the blend and multilayer films from WAXD pole figures and FT-IR are shown in Fig. 12. PP-2 shows *c*-axis orientation in MD and *b*-axis orientation perpendicular to MD (located in TD–ND plane) for both the blend and multilayer film, as was similarly observed for

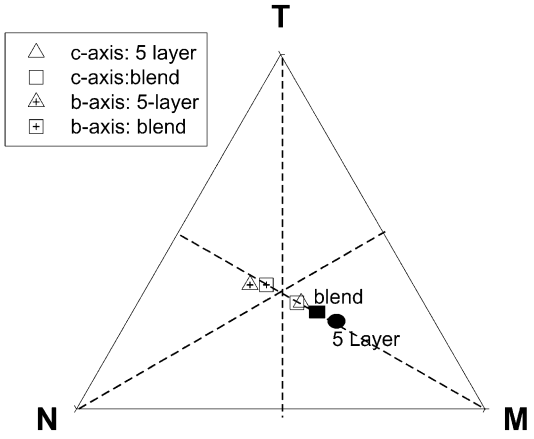

Fig. 12. Orientation functions obtained from X-ray (open symbols) and from FT-IR (filled symbols, *c*-axis only) for the PP-2 components in blends and 5-layer films.

PP-1 above. This indicates basically a similar structure for the PP phase, for both homopolymer and copolymer, in all films systems, whether it is pure PP, a blend with LLDPE or a multilayer film with LLDPE.

The LLDPE orientation in PP-2/LLDPE systems is shown on Fig. 13. The LLDPE in multilayer film shows the same orientation trend as pure LLDPE does: *a*-axis orientation toward MD, *b*-axis in TD–ND plane and *c*-axis in MD–TD plane. In the blend film, however, the *b*- and *c*-axes orientations are similar to those of the multilayer and pure films, whereas the *a*-axis orientation is observed in the ND–MD plane. This is probably due to a transcrystalline structure at the interface as discussed below and is significantly different from the PP-1 blend case above in which *a*-axis was in ND and *b*-axis in TD–MD, indicative of epitaxially grown structure.

In general, blends of PP and PE are known to be immiscible systems. The morphology for the film of LLDPE/PP-2 blend is shown in Fig. 14. Some transcrystallization zone around the interface can be easily

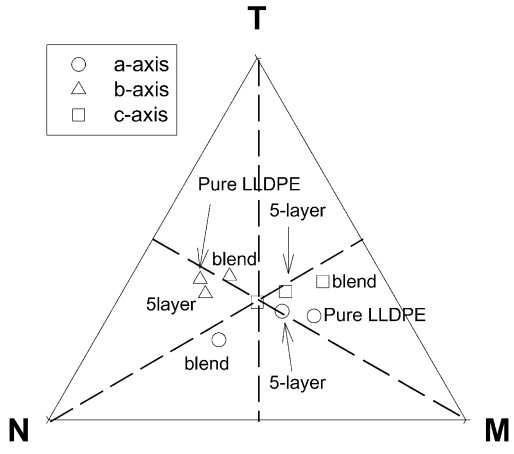

Fig. 13. The orientations of crystalline phases of PE component in the blend and 5-layer films using PP-2. Measured by FT-IR.

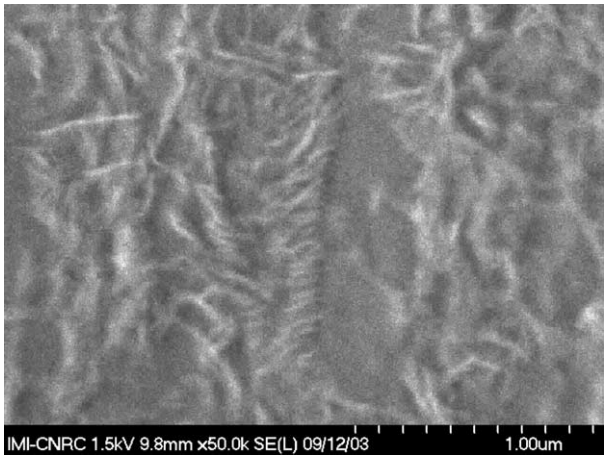

Fig. 14. Morphologies of LLDPE/PP-2 blend at composition of 50% LLDPE.

distinguished, they are PE lamellae nucleated on the first crystallized PP-2. No cross-hatched orientation is observed. The FT-IR orientation results for LLDPE are consistent with these morphological observations.

For the LLDPE/PP-2 5-layer film, its morphology is shown on Fig. 15. The crystallization of PE overgrows at the interfaces. In the vicinity of the PP-2, PP-2 triggered transcrystallization of LLDPE at the interface instead of the PP-initiated epitaxial orientation. These transcrystalline zones are always in the PE side, ranging between 60 and 150 nm. When PP-1 (homopolymer) is used instead of PP-2 (copolymer), no transcrystalline zone was observed as shown above. Transcrystalline layer is formed when a large number of nuclei are formed on an interface such that the crystallites are forced to grow normal to the interface and when a larger difference in crystallization temperature is present, which is the case between LLDPE and PP-2 (Table 1).

4. Conclusions

Two types of oriented lamellar structure may form at the interface for LLDPE/PP films: (1) a cross-hatched epitaxial crystalline structure, in which PE show an epitaxial arrangement crystallizing on oriented α-PP substrate, with their chains oriented at an angle of about 50° apart from i-PP chain direction; (2) a transcrystalline structure: the polymer with higher crystallization temperature induces an oriented crystallization of the lower crystallization temperature phase, this generates an increased number of nuclei at the interface and a particular orientation in the interfacial region. LLDPE/PP-1 (homopolymer) system showed epitaxial crystallization of LLDPE on oriented PP-1 in MD–TD plane, with no transcrystalline zone or epitaxial crystallization in thickness direction. LLDPE/PP-2 (copolymer) blend and multilayer film showed a clear transcrystalline overgrowth of LLDPE on PP at the interface, but no cross-

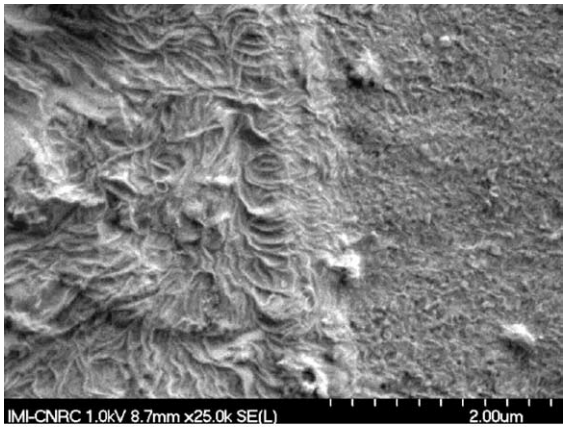

(a)

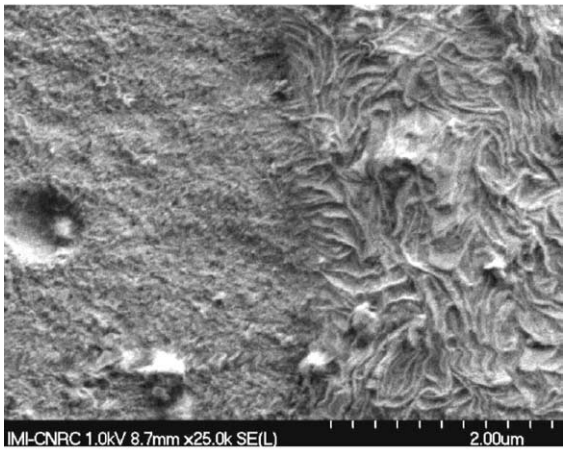

(b)

Fig. 15. Morphologies of LLDPE/PP-2 5-layer film: (a) left side, (b) right side.

hatched epitaxial crystal was found in this blends. LLDPE tended to crystallize on oriented isotactic PP homopolymer in epitaxial growth in the film plane.

The presence of this layer at the interface may contribute toward the improvement of adhesion. It has been found that epitaxial crystallization was helpful in enhancing the interfacial adhesion at the interface of two crystalline polymers.

References

[1] Garber CA, Clark ES. J Macromol Sci Phys 1970;B4:499.
[2] Hill MJ, Keller AJ. J Macromol Sci Phys 1969;B3:153. Hill MJ, Keller AJ. J Macromol Sci Phys 1971;B5:591.
[3] Keller A, Kolnaar HWH. Flow induced orientation and structure formation. In: Meijer HEH, editor. Processing of polymer, vol. 8. New York: VCH; 1997.
[4] Kumaraswamy G, Verma RK, Issaian AM, Wang P, Kornfield JA, Yeh F, et al. Polymer 2000;41:8931–40.
[5] Chatterjee AM, Price FP, Newmann SJ. J Polym Sci Polym Phys Ed 1975;13:2369 [also see p. 2385 and 2391].
[6] Wittman JC, Lotz B. Prog Polym Sci 1990;15:909.
[7] Yan S, Yang D, Petermann J. Polymer 1998;39:4569.
[8] Lotz B, Wittmann JC. J Polym Sci Polym Phys Ed 1986;24:1559.
[9] Tao X, Yan S, Yang D. Chin Chem Lett 1993;12:1093.
[10] Wittmann JC, Lotz B. J Polym Sci Polym Phys Ed 1985;23:205.
[11] Yan S, Petermann J. J Polym Sci: Part B Polym Phys 2000;38:80–3.
[12] Binsbergen FL. J Polym Sci Polym Phys Ed 1970;8:1545.
[13] Gray DG. J Polym Sci Polym Lett Ed 1974;12:645.
[14] Hobbs SY. Nat Phys Sci 1972;239:28.
[15] He T, Porter RS. J Appl Polym Sci 1988;35:1945.
[16] Zhang XM, Verilhac JM, Ajji A. Polymer 2001;42:8179.
[17] Zhang XM, Elkoun S, Ajji A, Huneault MA. Polymer 2004;45:217.
[18] Parthasarthy G, Sevegney M, Kannan RM. J Polym Sci: Part B Polym Phys 2002;40:2539–51.
[19] Painter PC, Watzek M, Koenig JL. Polymer 1977;18:1169–72.
[20] Tadokoro H, Kobiyashi M, Ukita M, Yasufuku K, Murahashi S, Torii T. J Chem Phys 1965;4:1432–49.
[21] Song Y, Nitta KH, Nemoto N. Macromolecules 2003;36:1955–61.
[22] Samuels RJ. J Polym Sci: Part A 1965;3:1741–63.
[23] Cole KC, Ajji A. Orientation characterization in polypropylene. In: Karger-Kocsis J, editor. Polypropylene an A–Z reference. Dordrecht, The Netherlands: Kluwer Academic Publishers; 1999.
[24] Ajji A, Zhang X, Elkoun S. Polymer 2005 in press.
[25] Whilchinsly ZW. J Appl Phys 1959;30:792.
[26] Chang AC, Tau L, Hiltner A, Baer E. Polymer 2002;43:4923–33.
[27] Asano T, Yan S, Petermann J, Yoshida S, Tohyama N, Imaizumi K, et al. J Macromol Sci: Part B Phys 2003;B42:489–97.
[28] Kestenbach HJ, Loos J, Petermann J. Polym Eng Sci 1998;38:478.